Proceedings of 2010 LWR Fuel Performance/TopFuel/WRFPM
Orlando, Florida, USA, September 26-29, 2010
Paper 0116

PWR TRANSIENT XENON MODELING AND ANALYSIS USING STUDSVIK CMS

Magnus Kruners [a], Gerardo Grandi [b], Mattias Carlsson[c]
[a)] *Studsvik Scandpower AB, Stenåsavägen 34, Varberg, Sweden*
Tel: +46 (0)340 13506, Email: Magnus.Kruners@studsvik.com
[b)] *Studsvik Scandpower Inc, 504 Shoup Avenue, Suite 201, Idaho Falls, ID 83402, USA*
Tel: +1 208 528 2398, Email: Gerardo.Grandi@studsvik.com
[c)] *Ringhals AB (Vattenfall), 432 85 Väröbacka, Sweden*
Tel: +46 (0)340 667477, Email: mattias1.carlsson@vattenfall.com

Abstract – *PWR core instabilities, due to axial xenon oscillations, are very important both in the core design phase and during plant operation. Core stability calculations depend on the accurate evaluation of the feedback mechanisms: Doppler coefficient, computed by the lattice physics code, and on the nodal fuel temperature and moderator density distributions computed by the steady state code. This paper contains the results of typical PWR transient scenarios for which the core stability and axial xenon transients have been assessed. Such core follow axial xenon transients have been studied by means of the Studsvik CMS code package (CASMO5 and SIMULATE5). SIMULATE5 calculations have been performed for the Ringhals-2, Ringhals-3 and Ringhals-4 (PWRs) over a wide range of operating conditions – including detailed load follow and coast down operation. The more negative Doppler coefficient predicted by CASMO5 and the fuel temperatures computed by SIMULATE5 result in good agreement with plant data during xenon transients.*

I. INTRODUCTION

Ringhals AB is a Swedish nuclear power site with four reactors units, three pressurized water reactors and one boiling water reactor. It is situated on the Värö Peninsula in Varberg Municipality approximately 60 km south of Gothenburg. With a total power rating of 3560 MWe, it is the largest nuclear power site in Sweden and generates 24 TWh of electricity a year, the equivalent of 20% of the electrical power usage of Sweden. Ringhals AB is owned 70% by Vattenfall and 30% by E.ON. All units in Ringhals operate in typical 12 month cycles, the three PWRs all of Westinghouse 3 loop design, represent two generations:

- Ringhals 2: 157 assemblies of 15 by 15 fuel pins design, originally constructed for a rated power of 2432 MW_T power up rated in 1989 to 2652 MW_T.
- Ringhals 3 and 4: 157 assemblies of 17 by 17 fuel pins design, originally constructed for a rated power of 2775 MW_T. Ringhals 3 up rated in 2006 to 2992 MW_T and in 2008 to 3135 MW_T.

All three PWRs at Ringhals are loaded according to low leakage loading pattern (LLLP), no fresh in peripheral position of the core. Figure 1 illustrates two examples of load following on Ringhals 2 cycle 16.

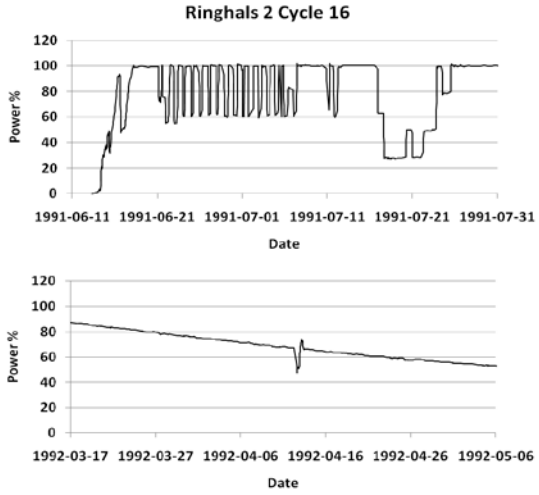

Fig. 1. Typical Ringhals 2 load follow.

The upper one, during the first part of the cycle, "day and weekend load follow", the lower plot an example of cost down load follow, down power during night hours to then boost some extra power out at morning hours by using xenon deficit. All units at Ringhals (BWR and PWR) as well as rest of the NPP in Sweden are utilized in load follow operations if so demanded by the national grid operator.

I.A. Sensitiveness to axial xenon oscillations

The fuel loaded in the Ringhals PWRs has in this study, an enrichment in the range of 3.40 – 3.95 wt % ^{235}U. About one quarter of the core is replaced per cycle (36 – 44 fuel assemblies) around half of those assemblies without Gd.

The relatively low enrichment, in combination with a flat or slightly double humped axial power distribution, do often results in cores that are highly sensitive to xenon oscillations. Fig. 2 shows the measured power and delta flux[a] (DI) during a load follow close to BOC. Fig. 3 shows the same quantities during the coast down starting at EOFP 100% power (226 EFPD from BOC) and ending 44 days later at 69% power. Both cases show a tendency towards axial power shape oscillations.

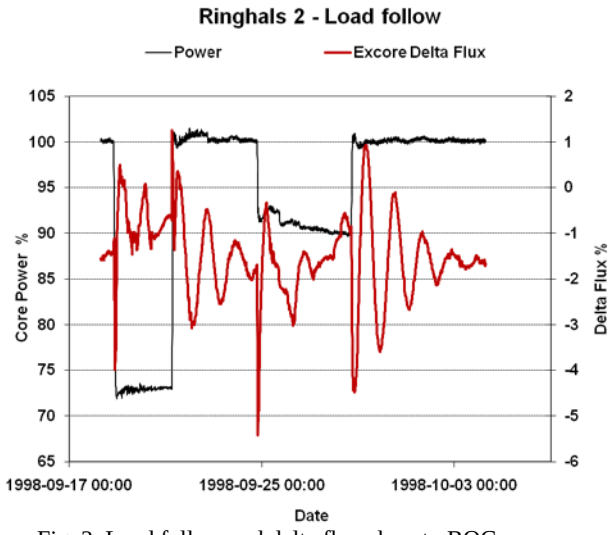

Fig. 2. Load follow and delta flux close to BOC.

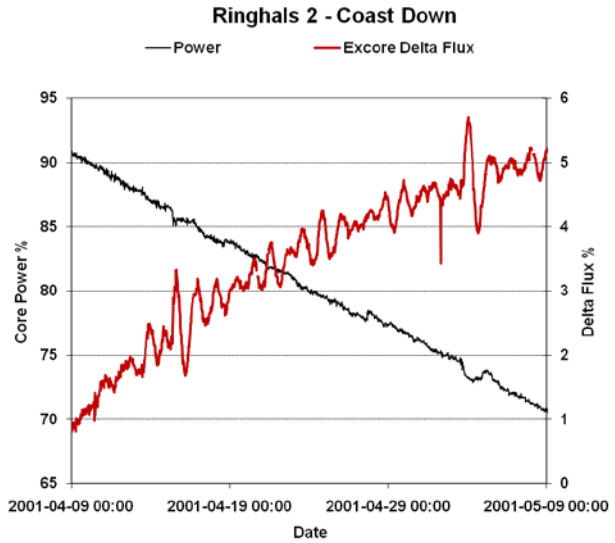

Fig. 3. Power and delta flux during coast down.

[a] DI % is the axial offset times core power in %

I.B. Operational support/guidance

To provide support and guidance for operating cores that are highly sensitive to xenon induced axial power oscillations, the reactor engineer needs an accurate in-core fuel management (ICFM) system.

Two ICFM systems will be considered in what follows, namely: 'C4/IP3/S3' and 'C5/S5'. 'C4/IP3/S3' is shorthand for the old generation of CMS codes (CASMO-4 (C4) [1], INTERPIN-3 (IP3) [2], and SIMULATE-3 (S3) [3]), while 'C5/S5' designates the new generation of CMS codes CASMO5 (C5) [4] and SIMULATE5 (S5) [5].

Differences between these two ICFM systems, relevant for PWR transients, will be described in this paper. CASMO5 developments, which have a significant impact on the fuel temperature coefficient, are discussed in Section II. The SIMULATE5 fuel pin model is described in Section III. Section III includes a comparison of SIMULATE5 predicted centerline temperatures against Halden experimental data is included.

CASMO5's more faithful modeling of the fuel temperature coefficient, together with the SIMULATE5 fuel temperature calculation, bring significant improvements in the prediction of PWR transients. Extensive 'C5/S5' predictive calculations were performed for Ringhals PWRs over a wide range of operating conditions. A few examples of such calculations will be discussed in Section IV.

II. FUEL TEMPERATURE COEFFICIENT

CASMO5 has many new features compared with its predecessor CASMO-4. Among them, the replacement of the L-library (based primarily on ENDF/B IV data) by the latest available nuclear data (ENDF/B VII.0) [4], and the correct treatment of the ^{238}U resonance treatment [6] have a significant impact on the fuel temperature coefficient (FTC).

Table I and Figure 4 illustrate the FTC for one of the 15 by 15 UO_2 lattices with a 3.6% enrichment used in the present work.

TABLE I

Comparison of the FTC for a UO_2 lattice at 20 GWd/T

Temperature [K]	CASMO-4 [pcm/K]	CASMO5 [pcm/K]
800	-2.57	-2.89
900	-2.40	-2.75
1000	-2.30	-2.66
1100	-2.22	-2.58
1200	-2.14	-2.46

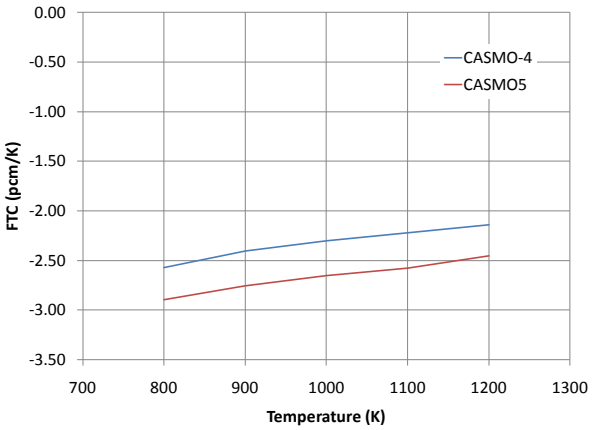

Fig. 4. Comparison of FTC for UO_2 lattice.

Results from Table I show that the Doppler coefficient predicted using CASMO5 cross section data is ~12% more negative than CASMO-4 cross section data. It is interesting to mention that the proper treatment of the ^{238}U resonance elastic scattering is the main contributor to the more negative Doppler coefficient [7]. Results in Section IV will show that the more negative fuel temperature coefficient computed by CASMO5 has a significant impact on the damping of axial power oscillations during xenon transients.

III. FUEL TEMPERATURE

SIMULATE5, Studsvik's next generation nodal code, has been developed to address the challenges of advanced core designs with increased heterogeneity and aggressive operating strategies. S5 relies on detailed modeling of the fuel assembly geometry taking into account the complicated mix of fuel enrichment zones, control rod zones, and spacer grids. One of the differences between SIMULATE5 and its predecessor SIMULATE-3 for PWR cores is the thermal-hydraulics (TH).

S5 PWR TH which can model each of the assemblies in the core has an active channel and a number of parallel water rods [8]. S5 offers two ways to compute the PWR assembly flow distribution. The '1D' model assumes that radial cross flow can be neglected. The advanced cross flow model allows assembly or nodal cross flow. The S5 cross flow model is close to that of the COBRA IIIC [9] code with balance equations for flow rate, energy, axial momentum, and lateral momentum.

The 3D fuel temperature distribution is evaluated in the TH module by solving the one-dimensional, heat conduction equation for the average fuel pin of each node instead of relying on pre-computed fuel temperature tables.

The SIMULATE5 fuel pin model is based on models derived from the INTERPIN-4 code [10]. The fuel and cladding thermal conductivities are temperature and burnup dependent. Different sets of correlations are provided for UO_2 and MOX fuel. The closure of the gap between the cladding and the fuel pellet plays an important role in the determination of the gap conductivity. The following physical effects for the gap are modeled: (a) fuel pellet cracking, (b) fuel pellet irradiation swelling, (c) fuel pellet and clad thermal expansion, (d) clad compression caused by irradiation at high temperature and (e) gas gap composition changes as a result of fission gas release. The radial distribution of the volumetric heat source in the pellet is dependent on the fuel depletion. The radial power profiles have been computed with CASMO5 for typical UO_2 and MOX pins. The channel TH model provides the coolant temperature surrounding the pins as the boundary condition for the fuel temperature calculation.

III.A. Comparison with HALDEN data

Table II summarizes the relevant geometry data of the fuel pins from the Halden experimental program [11-12] that have been chosen for the validation of the SIMULATE5 fuel pin model. These tests were chosen as part of the assessment of the INTERPIN-3 code many years ago. It is important to mention that the centerline temperatures in these tests do not exceed the fission gas release threshold. This ensures that the conditions are prototypical of normal operating conditions.

TABLE II

Geometry of the fuel rods from Halden

IFA #	Rod #	Diameter of Pellet / Thermocouple hole (mm)	Fuel-cladding diametral gap (μm)
432	3	10.850 / 1.80	70
504	1	10.590 / 1.80	200
505	924D	10.700 / 1.80	100
515_11	A1	5.560 / 1.80	50
552	6	8.040 / 1.80	180
552	7	8.090 / 1.80	130
562.1	6	10.590 / 2.04	70
562.2	15	5.915 / 2.00	100

For the purpose of centerline temperatures comparisons, the measured data have been corrected to a constant linear heat generation rate. This removes the influence of the actual pin and reactor power history from the comparisons, without significantly increasing the uncertainty in the measurements. The fuel centerline temperatures for these measurements were made with conventional thermocouples or expansion thermometers. Experimental uncertainties on measured fuel temperatures are quoted to be 50-70 K.

Table III compares S5 centerline temperatures against experimental data in term of bias and standard deviation. Figs. 5 and 6 compare S5 centerline temperatures (blue line) against experimental data (red line) as a function of exposure for IFA 504 rod 1 and IFA 562 rod 15 respectively.

TABLE III

Bias and standard deviation of SIMULATE5 centerline temperatures

IFA #	Rod #	Bias (K)	Std. Deviation (K)
432	3	+63	10
504	1	-29	34
505	924D	-1	38
515_11	A1	-69	12
552	6	-77	10
552	7	-87	9
562.1	6	58	27
562.2	15	50	9
Mean Value		-12	19

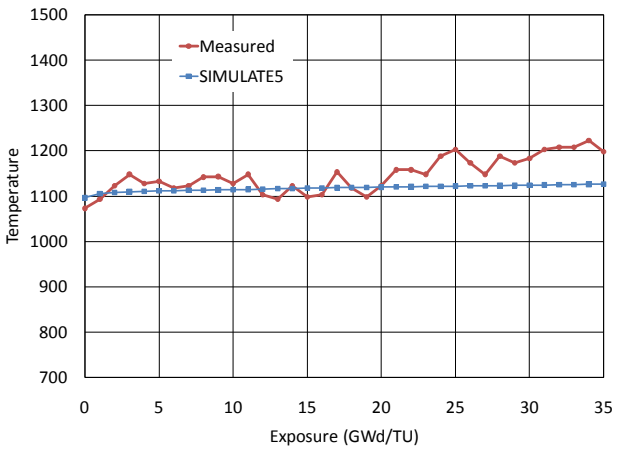

Fig. 5. Centerline fuel temperature for IFA 504 rod 1.

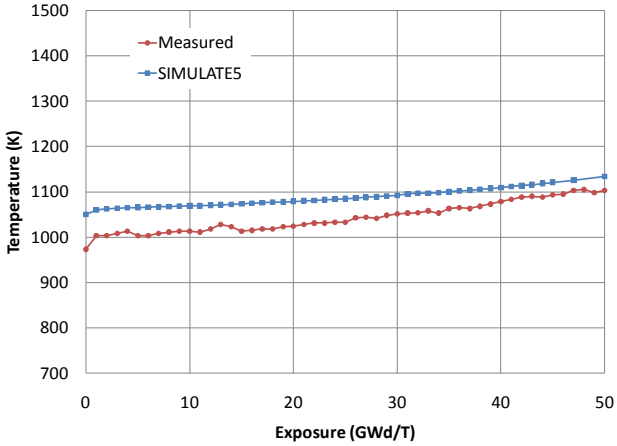

Fig. 6. Centerline fuel temperature for IFA 562 rod 15.

SIMULATE5 results show good agreement with experimental data.

III.B. Comparison of SIMULATE5 and INTERPIN-3 effective Doppler temperatures

In steady state, the intra-pellet fuel temperature distribution is almost a quadratic function of the radial position. However, the cross sections computed by CASMO5 assume a flat fuel temperature profile in the pellet. The steady state nodal simulator must calculate an "effective Doppler temperature" for the cross section evaluation.

Grandi et al. [7], discuss several effective Doppler temperature (T_{EFF}) definitions available in the literature and propose a weighted average of the volume-averaged temperature (T_{AVG}) and the surface temperature (T_S),

$$T_{EFF} = \omega \cdot T_{AVG} + (1-\omega) \cdot T_S \qquad (1)$$

where the value of ω (0.92) has been empirically adjusted to match the Doppler feedback between hot zero and hot full power cases computed by Monte Carlo calculations.

Figure 7 compares the effective fuel temperature computed by IP3 and S5 as a function of exposure for one of the 15 by 15 UO_2 lattices. The linear heat generation rate was set to 22.6 kW/m in order to represent core rated power conditions. It is important to mention that while IP3 defines the effective Doppler temperature as the volume-averaged temperature (T_{AVG}), S5 uses the value defined by Eq. (1).

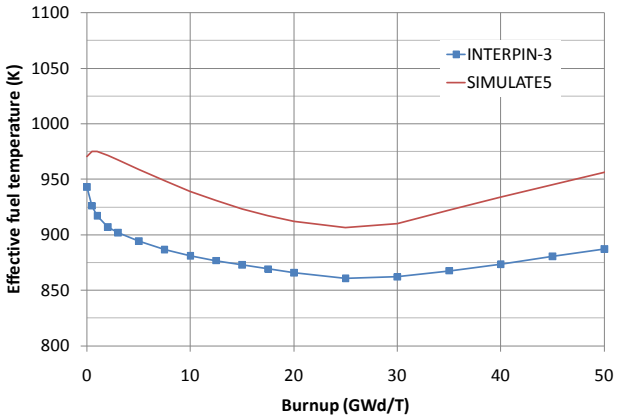

Fig. 7. Effective Doppler temperature comparison.

Note that S5 effective Doppler temperatures are higher than the ones computed by IP3. Differences are mainly due to an improvement in the gaseous gap conductance model that accounts for the roughness of fuel pellet outer and inner cladding surfaces.

Fig. 8 shows the effective Doppler temperature derivative when the linear heat generation rate changes from 11.3 kW/m to 45.2 kW/m.

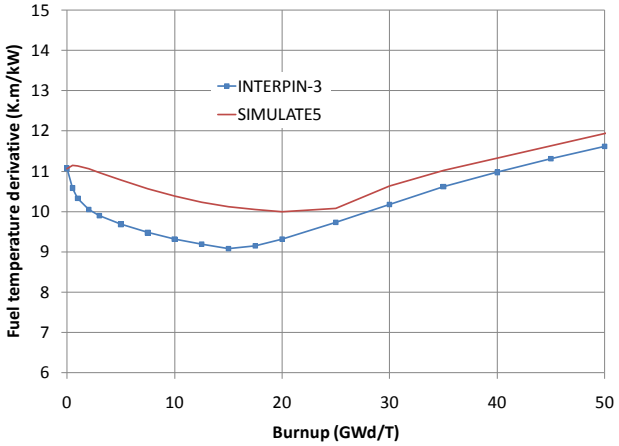

Fig. 8: Fuel temperature increase.

Note that temperature change computed by S5 is always equal or greater than the changes computed by IP3.

IV. TRANSIENT RESULTS

Transient calculations rely on the accurate evaluation of the fuel and moderator temperature feedback on the cross section evaluation as computed by the lattice physics code, and on the nodal pin fuel temperature and moderator density distributions computed by the steady state code.

In particular, the Doppler reactivity ($\Delta\rho_D$) is proportional to the FTC and the derivative of the effective Doppler temperature (T_{EFF}) with respect to power (P),

$$\Delta\rho_D \propto FTC \cdot \frac{\partial T_{EFF}}{\partial P} \cdot \Delta P \qquad (2)$$

The more negative Doppler temperature coefficient computed by CASMO5 (see Fig. 4), and the higher effective Doppler temperature derivative (see Fig. 8) are compounded to provide more reactivity feedback during xenon transients. Some cases from the extensive SIMULATE5 predictive calculations performed for Ringhals 2 are discussed in what follows, illustrating the effect of the more negative Doppler feedback on axial power oscillations.

Fig. 9 is similar to Fig. 2, but now "C4/IP3/S3" and "C5/S5" results have been added. The results are based on 4603 cases, calculated with a frequency of one case every five minutes during the transient. The calculated DI has been adjusted by the average bias between the calculated DI result and measured DI from the first 155 constant full power cases. For 'C4/IP3/S3' a bias of +0.600 has been used, and for 'C5/S5' a bias of -0.026.

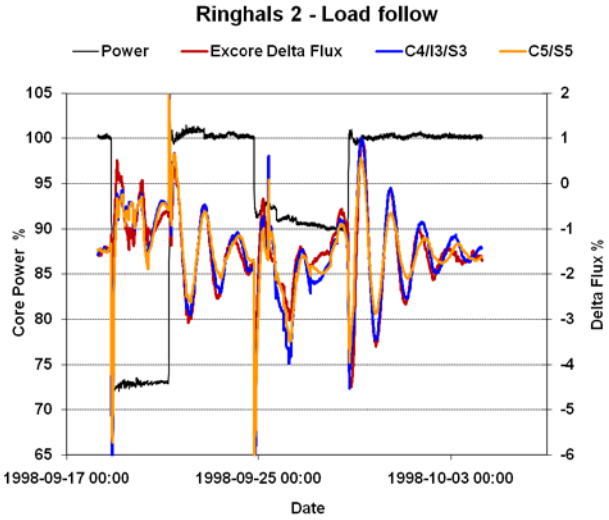

Fig. 9. Ringhals-2 load follow close to cycle 16 BOC.

Figure 9 results may lead to the false conclusion that 'C5/S5' do not provide any improvement for PWR operation support. However, improvements are well illustrated by the coast down calculation starting at EOFP 100% power (226 EFPD from BOC) and ending 44 days later at 69% power. Results are summarized in Figs. 10 and 11 in terms of delta flux.

Results in Figs. 10 and 11 are based on 2114 cases with a frequency of one case every 30 minutes during the coast down period. The calculated DI has been adjusted by

the average bias between the calculated DI result and measured DI from the first 100 cases in the series. Biases of -1.053 and -1.751 have been used for 'C4/IP3/S3' and 'C5/S5', respectively. It is important to mention that:

- The Y-axis to the right has been rescaled compared to Fig. 3.
- The X-axis start and ending date is a part/window of the full covered/calculated period. This gives the impression that the calculated and bias adjusted DI is not correct in Fig. 10. Fig. 11 shows the same results for the first 10 days of the coast down and the bias adjusted calculated DI could therefore be confirmed.

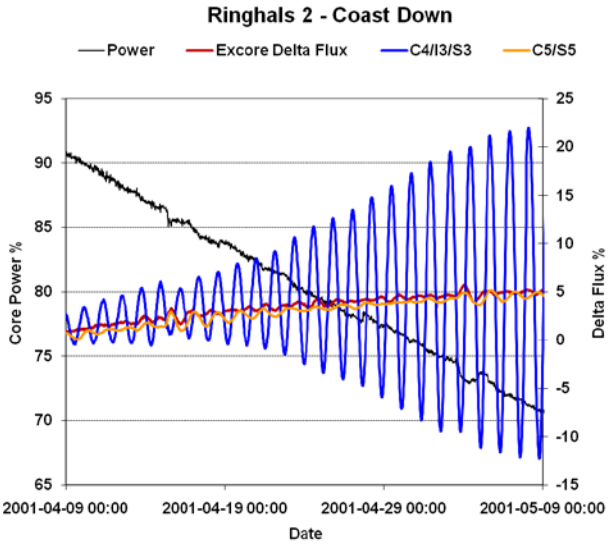

Fig. 10. . Ringhals 2 cycle 16 coast down.

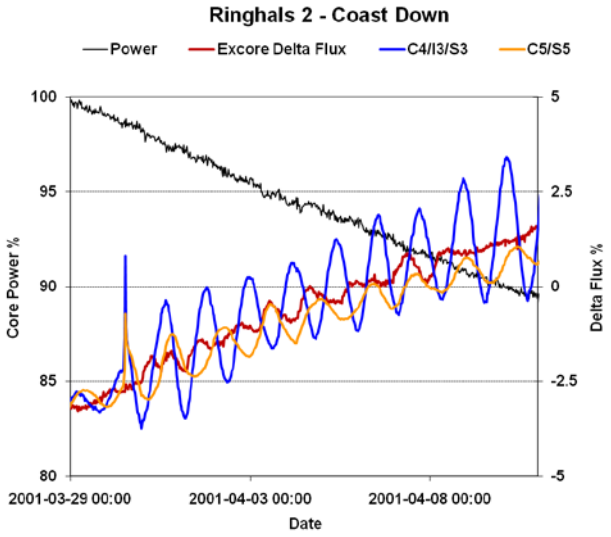

Fig. 11. Ringhals 2 cycle 16 coast down (first 10 days).

Note that while the measured plant data is smooth, the 'C4/IP3/S3' calculation shows large axial power swings which are symptomatic of under-damped xenon transients. The 'C5/S5' calculations are in good agreement with the measurements.

An accurate prediction of xenon transient behavior is important to operational control, particularly at EOC where boration/dilution capability is lacking and a double humped axial power shape may exist. As shown, transient xenon calculations are highly dependent on accurate modeling of the Doppler temperature coefficient and fuel temperature dependence with exposure. Results of C5/S5 show accurate ability to predict xenon transients, particularly towards EOC, as evidenced by Figs 10 and 11.

Figs. 12 and 13 compare measured and calculated delta flux during MOC load follow calculations (one case per every five minutes in cycles 25 and 26, respectively.

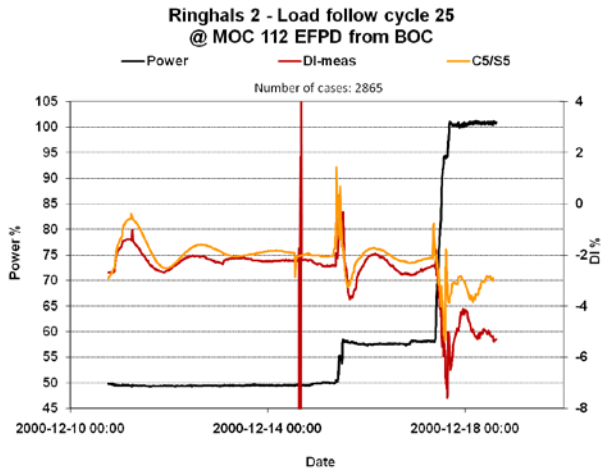

Fig. 12. Ringhals-2 cycle 25 MOC load follow.

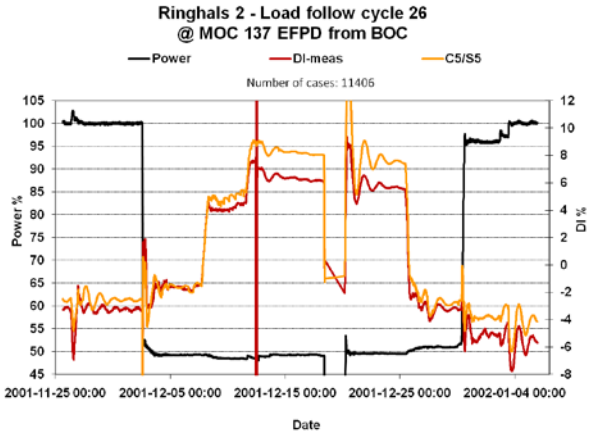

Fig. 13. Ringhals-2 cycle 26 MOC load follow.

Good agreement is shown between calculations and measurements. Note that the 'C5/S5' solution is neither over damped nor under damped.

Ringhals PWRs have high sensitivity to axial xenon oscillations during coast down calculations as shown in

Fig. 10. Therefore, further 'C5/S5' calculations were performed to assess their accuracy under such conditions. Figure 14 compares the measured (black line) and the calculated (blue or yellow line) power evolution using forced search estimated power calculations to simulate the cycle 25 coast down.

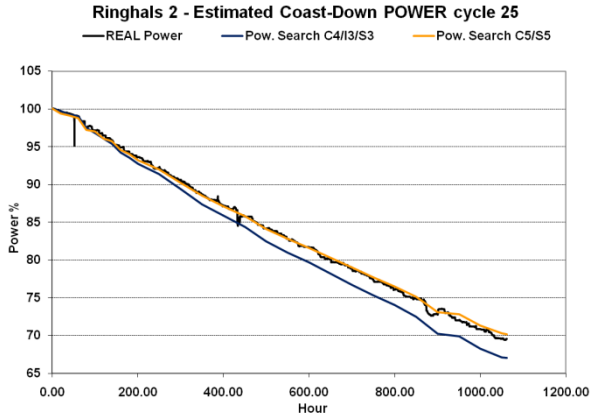

Fig. 14. Ringhals 2 cycle 25 coast down power.

From Fig. 14 it is clear that the new code combination, CASMO5 and SIMULATE5, predicts a better projection of total core power during the slow coast down. So, even for this kind of slow power transient, the new codes, with improved fuel temperature calculation and Doppler reactivity feedback, do result in a more accurate prediction of total core power. From Fig. 14 we could see that the power difference at end of coast down will be 70.3% (C5/S5) and 67.1% (C4/I3/S3) compared to a real power of 69.6%.

Figure 15 compares the measured (red line) and the calculated (yellow line) delta flux (one case per every 30 minutes).

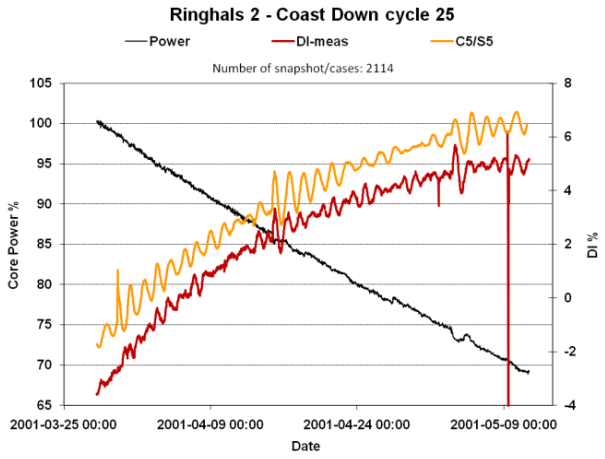

Fig. 15. Ringhals 2 cycle 25 coast down power.

The main conclusion from Figs. 14 and 15 is that CASMO5 and SIMULATE5 are able to accurately predict both power and the axial power shape which result from the xenon transient during coast down.

VI. CONCLUSIONS

Results presented in this paper clearly show that the combination of CASMO5 and SIMULATE5 can accurately predict PWR xenon transients from BOC to coast down. Calculations do not show either diverging or over damped results.

Improvements in the axial power shape predictions have been observed and are due to:

- The more negative fuel temperature coefficient computed by CASMO5 as a result of the proper treatment of the ^{238}U resonance elastic scattering treatment.
- The higher effective Doppler temperature derivative with respect to power due to improvements in the gaseous gap conductance model supported by Halden experimental data.

The work presented here is part of an ongoing research project at Studsvik to evaluate CASMO5 / SIMULATE5 as an ICFM tool that provides support and guidance to the reactor engineer and/or its implementation in a core supervision system such as GARDEL [13].

ACKNOWLEDGMENT

SSP authors want to specifically thank Vattenfall Sweden and Ringhals AB for their kind support. Both organizations willingly assisted SSP with data and operating histories in high detail for many cycles and power variations from all three PWRs at Ringhals.

REFERENCES

1. K. SMITH and J. RHODES, "CASMO-4 Characteristic Methods for Two Dimensional PWR and BWR Core Calculations," *Trans. Am. Nucl. Soc.*, **83**, 322 (2000).

2. D. HAGRMAN, "INTERPIN-3 User's Manual," Studsvik Scandpower, Inc. Report SSP-01/430 (2001).

3. D. DEAN and K. REMPE, "SIMULATE-3 User's Manual," Studsvik Scandpower, Inc. Report SSP-95/15 Rev. 3 (1995).

4. J. RHODES, et al., "CASMO-5 development and Applications," *Advances in Nuclear Analysis and Simulation (PHYSOR 2006)*, Vancouver, BC, Canada (2006).

5. T. BAHADIR, S-Ö LINDAHL, "Studsvik's Next Generation Nodal Code SIMULATE-5", *Advances in Nuclear Fuel Management IV (ANFM 2009)*, Hilton Head Island, South Carolina, USA (2009).

6. D. LEE, et al., "The Impact of 238U Resonance Elastic Scattering Approximations on Thermal Reactor Doppler Reactivity," *Annals of Nuclear Energy*, **36**, pp. 274-280 (2009).

7. G. GRANDI, et al., "Effect of CASMO-5 Cross Section Data and Doppler Temperature Definitions on LWR Reactivity Initiated Accidents," *Advances in Reactor Physics to Power the Nuclear Renaissance (PHYSOR 2010)*, Pittsburgh, USA (2010).

8. S-Ö LINDAHL, et al., "SIMULATE-4 developments", *Nuclear Power: A Sustainable Resource (PHYSOR 2008)*, Interlaken, Switzerland (2008).

9. S. ROWE, "COBRA III-C: A Digital Computer Program for Steady State and Transient Thermal-Hydraulic Analysis of Rod Bundle Nuclear Fuel Elements", BNWL-1695 (1973)

10. G. GRANDI and D. HAGRMAN, "Improvements to the INTERPIN code for High Burnup and MOX fuel," *Trans. Am. Nucl. Soc*., **97**, 614 (2007).

11. G. KJAERHEIM and E. ROLDSTAD, "In pile determination of UO2 thermal conductivity, density effects and gap conductance", HPR 80, Halden, Norway, (1967).

12. E. KOLSTAD and F. SONTHEIMER, "Fuel Thermal Conductivity Changes with Burnup as Derived from In-Pile Temperature measurements," HWR-299, Halden, Norway (1991).

13. A. NOËL and D. DEAN, "GARDEL BWR On-line Monitoring Experience at Cooper and Monticello," *Trans. Am. Nucl. Soc*. **97**, 737-738, November (2007).